

1 Partitioning uncertainty in projections of Arctic sea 2 ice

3 **David B. Bonan**

4 Environmental Science and Engineering, California Institute of Technology, Pasadena, California

5 E-mail: dbonan@caltech.edu

6 **Flavio Lehner**

7 Department of Earth and Atmospheric Science, Cornell University, Ithaca, New York
8 Climate and Global Dynamics Laboratory, National Center for Atmospheric Research, Boulder,
9 Colorado

10 **Marika M. Holland**

11 Climate and Global Dynamics Laboratory, National Center for Atmospheric Research, Boulder,
12 Colorado

13 **Abstract.** Improved knowledge of the contributing sources of uncertainty in
14 projections of Arctic sea ice over the 21st century is essential for evaluating impacts of
15 a changing Arctic ecosystem. Here, we consider the role of internal variability, model
16 structure and emissions scenario in projections of Arctic sea-ice extent (SIE) by using
17 six single model initial-condition large ensembles and a suite of models participating in
18 Phase 5 of the Coupled Model Intercomparison Project. For projections of September
19 Arctic SIE, internal variability accounts for as much as 60% of the total uncertainty
20 in the next few decades, while emissions scenario dominates uncertainty toward the
21 end of the century. Model structure accounts for approximately 70% of the total
22 uncertainty by mid-century and declines to 20% at the end of the 21st century. For
23 projections of wintertime Arctic SIE, internal variability contributes as much as 60% of
24 the total uncertainty in the first few decades and impacts total uncertainty at longer
25 lead times when compared to summer SIE. Model structure contributes the rest of
26 the uncertainty with emissions scenario contributing little to the total uncertainty. At
27 regional scales, the contribution of internal variability can vary widely and strongly
28 depends on the month and region. For wintertime SIE in the GIN and Barents Seas,
29 internal variability contributes approximately 70% to the total uncertainty over the
30 coming decades and remains important much longer than in other regions. We further
31 find that the relative contribution of internal variability to total uncertainty is state-
32 dependent and increases as sea ice volume declines. These results demonstrate the need
33 to improve the representation of internal variability of Arctic SIE in models, which is
34 a significant source of uncertainty in future projections.

35 Keywords: *sea ice, climate change, uncertainty*

36
37 Submitted to: *Environ. Res. Lett.*

38 1. Introduction

39 The rapid loss of Arctic sea ice over the last few decades has been one of the most iconic
40 symbols of anthropogenic climate change. Since the beginning of the satellite record,
41 September Arctic sea-ice extent (SIE) has decreased by approximately 50% (Stroeve
42 and Notz, 2018) and experienced considerable thinning largely due to a lengthening of
43 the melt season (Perovich and Polashenski, 2012; Stroeve et al., 2014). While state-of-
44 the-art global climate models (GCMs) predict a decline of Arctic SIE throughout the
45 21st century, the exact amount of ice loss remains highly uncertain (Massonnet et al.,
46 2012; SIMIP, 2020). Studies suggest that in the summertime the Arctic will most likely
47 be “ice free” by the end of the 21st century (Jahn, 2018; Niederdrenk and Notz, 2018;
48 Sigmond et al., 2018) and could possibly be ice free as early as 2050 (Jahn, 2018) or
49 2030 (Wang and Overland, 2009). To improve projections of Arctic sea ice, the rela-
50 tive importance of the sources of uncertainty need to be characterized and if possible
51 reduced, particularly at regional scales (Eicken, 2013; Barnhart et al., 2016).

52
53 Internal variability, which refers to natural fluctuations in climate that occur even in the
54 absence of external forcing, has long been known as an important source of uncertainty
55 in projections of future climate (Hawkins and Sutton, 2009; Deser et al., 2012, 2020;
56 Lehner et al., 2020; Maher et al., 2020). These fluctuations — intrinsic to the climate
57 system — have been shown to exert a strong influence on short-term trends in numer-
58 ous climate variables, such as surface temperature (Wallace et al., 2012; Smoliak et al.,
59 2015; Deser et al., 2016; Lehner et al., 2017), precipitation (Hawkins and Sutton, 2011;
60 Deser et al., 2012), snowpack (Siler et al., 2019), glacier mass balance (Marzeion et al.,
61 2014; Bonan et al., 2019), ocean biogeochemical properties (Lovenduski et al., 2016;
62 Schlunegger et al., 2020), and sea ice (Kay et al., 2011; Swart et al., 2015; Jahn et al.,
63 2016; Screen and Deser, 2019; Rosenblum and Eisenman, 2017; England et al., 2019;
64 Ding et al., 2019; Landrum and Holland, 2020). Recent estimates suggest that internal
65 variability has contributed to approximately 50% of the observed trend in September
66 Arctic SIE decline since 1979 (Stroeve et al., 2007; Kay et al., 2011; Zhang, 2015; Ding
67 et al., 2017, 2019) and has strongly controlled regional patterns of sea ice loss (England
68 et al., 2019).

69
70 The large role of internal variability in determining changes to Arctic SIE over the ob-
71 servational record means the predictability of future Arctic SIE at decadal timescales
72 could remain heavily influenced by internal variability. The advent of decadal predic-
73 tion systems (e.g., Meehl et al., 2009, 2014) raises the question whether realistic physics
74 together with proper initialization of observations can lead GCMs to successfully con-
75 strain this internal variability and result in skillful estimates of SIE at decadal lead times
76 (Koenigk et al., 2012; Yang et al., 2016). Initial-value predictability of Arctic SIE has
77 been shown to be regionally and seasonally dependent (Blanchard-Wrigglesworth et al.,
78 2011b; Bushuk et al., 2019), often only lasting a few years at most for total Arctic SIE

79 (Blanchard-Wrigglesworth et al., 2011a; Guemas et al., 2016). Using a suite of perfect
80 model experiments (which quantify the upper limits of predictability), Yeager et al.
81 (2015) showed that the rate of sea ice loss in the North Atlantic may slow down in the
82 coming decades due to a reduction of ocean heat transport into the Arctic, which itself
83 is highly predictable. Similarly, Koenigk et al. (2012) found a link between meridional
84 overturning circulation and the potential predictability of decadal mean sea ice concen-
85 tration in the North Atlantic — consistent with Yang et al. (2016). Indeed, this means
86 that uncertainty due to internal variability is an important — and possibly reducible —
87 source of uncertainty for short-term projections in some regions with properly initial-
88 ized forecasts, but not for long-term projections. However, even if uncertainty due to
89 internal variability cannot be reduced, understanding its magnitude will allow for better
90 decision making in light of that uncertainty. This raises an important question: what
91 is the relative role of internal variability in future projections of Arctic sea ice? Any
92 accounting for the sources of uncertainty in projections of Arctic SIE must quantify the
93 relative importance of each source at different spatial and temporal scales. For example,
94 how important is internal variability for projections of Arctic sea ice 15 versus 30 years
95 from now? Moreover, because models exhibit different magnitudes of internal variability
96 in sea ice, particularly at regional scales (e.g., England et al., 2019; Topál et al., 2020),
97 such quantification must sample the influence of model uncertainty in the estimate of
98 internal variability itself.

99

100 To examine these questions we use an unprecedented suite of single model initial-
101 condition large ensembles (SMILEs) from six fully-coupled GCMs. Due to their sample
102 size, these SMILEs uniquely allow us to partition uncertainty in projections of Arctic SIE
103 into the relative roles of internal variability, model structure, and emissions scenario at
104 both Arctic-wide and regional spatial scales without relying on statistical representations
105 of the forced response or internal variability (e.g., Lique et al., 2016). The SMILEs also
106 allow us to quantify the influence of different estimates of internal variability, a feature
107 of sea ice projection uncertainty that has received little attention. In what follows, we
108 first investigate the role of internal variability in projections of total Arctic SIE. We
109 then explore how the relative partitioning of each source changes as a function of season
110 and Arctic region and how this partitioning is influenced by the mean-state of Arctic
111 sea ice.

112 2. Data

113 2.1. MMLEA output

114 We use six SMILEs from the Multi-Model Large Ensemble Archive (MMLEA; Deser
115 et al., 2020) to investigate the role of internal variability on projections of Arctic
116 sea ice. These include the: 40 member Community Earth System Model Large
117 Ensemble Community Project (CESM1-LE; Kay et al., 2015), 50 member Canadian

118 Earth System Model Large Ensemble (CanESM2-LE; Kirchmeier-Young et al., 2017), 30
 119 member Commonwealth Scientific and Industrial Research Organisation Large Ensemble
 120 (CSIRO-Mk3.6.0-LE; Jeffrey et al., 2013), 20 member Geophysical Fluid Dynamics
 121 Laboratory Large Ensemble (GFDL-CM3-LE; Sun et al., 2018), 30 member Geophysical
 122 Fluid Dynamics Laboratory Earth System Model Large Ensemble (GFDL-ESM2M-LE;
 123 Rodgers et al., 2015), and 100 member Max Planck Institute Grand Ensemble (MPI-
 124 GE; Maher et al., 2019). Each SMILE uses historical and RCP8.5 forcing. We also
 125 use the RCP2.6 and RCP4.5 100 member ensembles from the MPI-GE. From each
 126 SMILE we use sea ice concentration (SIC) to compute monthly Arctic SIE (defined as
 127 the area where $SIC > 15\%$) for 6 Arctic regions and the pan-Arctic (see Figure S1). We
 128 also use sea ice thickness to compute monthly Arctic sea-ice volume (SIV) for these
 129 same spatial domains. Note that the output from GFDL-CM3 and GFDL-ESM2M is
 130 the average thickness over the ice-covered area of the grid cell. To compute SIV, the
 131 monthly averaged ice-covered thickness from both models was multiplied by the monthly
 132 average SIC of each cell to get the grid-cell average SIT. Prior to these calculations, all
 133 model output is regridded to a common $1^\circ \times 1^\circ$ analysis grid using nearest-neighbor
 134 interpolation.

135 2.2. CMIP5 output

136 We use monthly output from the historical, RCP2.6, RCP4.5, and RCP8.5 simulations
 137 of 30 different GCMs participating in CMIP5 (Taylor et al., 2012). Since the historical
 138 simulations end in 2005, we merge the 1850-2005 fields from the historical simulations
 139 with the 2006-2100 fields under each RCP forcing scenario. For each experiment, we
 140 use SIC to compute monthly Arctic SIE (defined as the area where $SIC > 15\%$). The set
 141 of GCMs evaluated reflects those that provide the necessary output (see Table S1). All
 142 model output is regridded to a common $1^\circ \times 1^\circ$ analysis grid using nearest-neighbor
 143 interpolation.

144 3. Uncertainty in projections of Arctic sea ice

We begin by partitioning three sources of uncertainty following Hawkins and Sutton (2009) and Lehner et al. (2020), where the total uncertainty (T) is the sum of the uncertainty due to model structure (M), the uncertainty due to internal variability (I) and the uncertainty due to emissions scenario (S). Each source can be estimated for a given time t and location x such that:

$$T(t, x) = I(t, x) + M(t, x) + S(t, x) \quad (1)$$

145 where the fractional uncertainty from a given source is calculated as I/T , M/T , and
 146 S/T . I is calculated as the variance across ensemble members of each SMILE, yielding
 147 one time-varying estimate of I per SMILE. Averaging across the six I yields the multi-
 148 model mean internal variability uncertainty (see white line in Figure 1). To quantify

149 the influence of model uncertainty in the estimate of I we also use the model with
150 the largest and smallest I (see white shaded regions in Figure 1). Model uncertainty
151 in the estimate of I has emerged as an important and potentially reducible source of
152 uncertainty in regional temperature and precipitation changes (Lehner et al., 2020; Deser
153 et al., 2020) and projections of global ocean biogeochemical properties (Schlunegger
154 et al., 2020). M is calculated as the variance across the ensemble means of the six
155 SMILEs. It is important to note that the SMILEs used in this study are found to be
156 reasonably representative of the CMIP5 inter-model spread for the percent of remaining
157 Arctic sea ice cover (see Figure S2) and total Arctic SIE (see black lines in Fig. 1), but
158 a more systematic comparison is necessary before generalizing this conclusion. Finally,
159 since only a few of the SMILEs were run with more than one emissions scenario, we turn
160 to CMIP5 for S , which is calculated as the variance across the multi-model mean RCP
161 scenarios (see Table S1 for details). Prior to these variance calculations, the monthly SIE
162 was smoothed with a 5-year running mean to isolate the effect of uncertainty on short-
163 term projections and then used to calculate the percent of remaining sea ice relative to
164 1995-2014 (see Figure S2).

165 3.1. Total Arctic sea-ice extent

166 We first consider projections of Arctic SIE in September (the seasonal minimum) and
167 March (the seasonal maximum). Figure 1 shows the fractional contribution of each
168 source of uncertainty to total uncertainty. In September, uncertainty due to internal
169 variability is important initially, accounting for approximately 30% of total uncertainty.
170 However, over time model uncertainty increases and eventually dominates for the first
171 half of the 21st century, before scenario uncertainty starts to dominate after approxi-
172 mately mid-century (Fig. 1c). However, model uncertainty in internal variability itself
173 can have an effect on climate projections (e.g., Lehner et al., 2020). Accounting for
174 the minimum and maximum contribution of internal variability to total uncertainty
175 suggests that internal variability could account for as much as 50-60% or as little as
176 10-20% of total uncertainty in projections of September SIE in the coming decades and
177 could contribute approximately 10% throughout the 21st century. Note, these results
178 are similar for most summer months and summertime averages (see Fig. S4 and S5).

179
180 A different story emerges for projections of Arctic SIE in March. While uncertainty
181 due to internal variability is again important initially and accounts for more of the total
182 uncertainty at longer lead times, model uncertainty increases and quickly dominates
183 until the end of the century (Fig. 1d). Scenario uncertainty is relatively less important
184 for projections of Arctic SIE in March and, more broadly, during the wintertime (see
185 Fig. S4). Uncertainty in model internal variability remains large throughout the 21st
186 century, suggesting internal variability could account for as much as 20% or as little as
187 5% of the total uncertainty beyond mid-century. The relative partitioning is similar for
188 most winter months and wintertime averages (see Fig. S4 and S5).

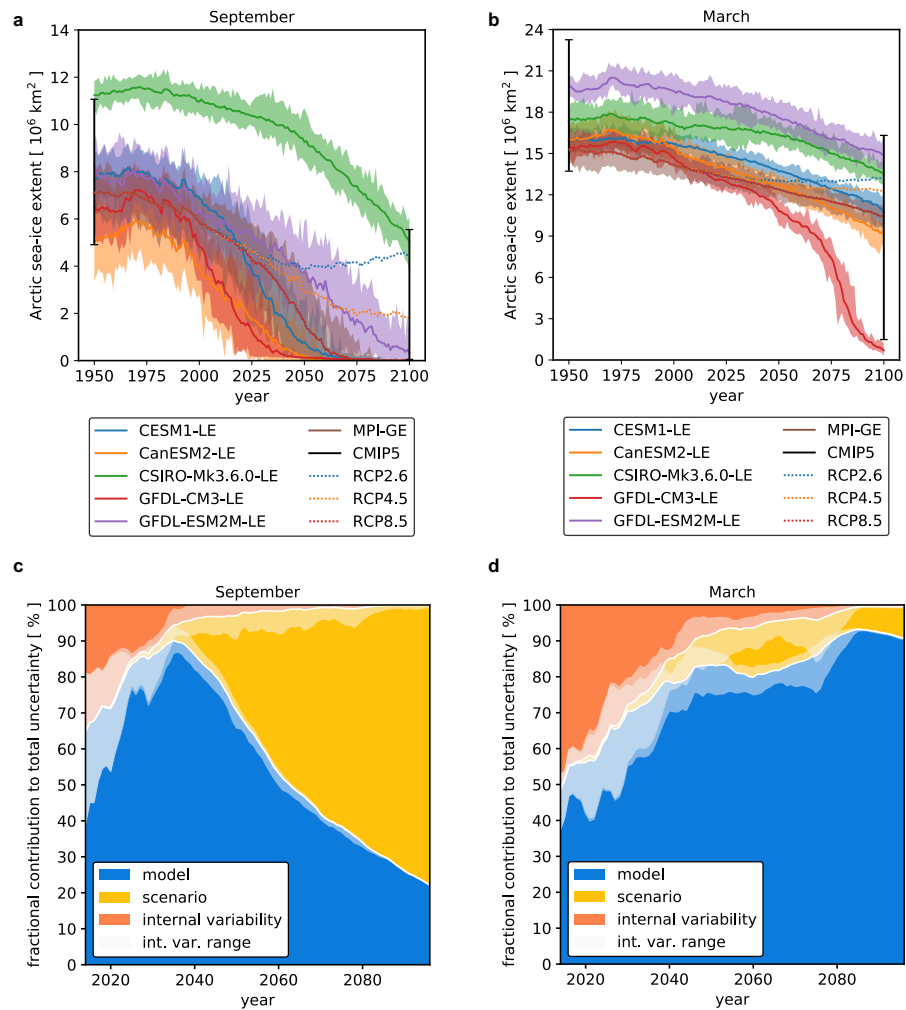


Figure 1. (a-b) Arctic sea-ice extent from 1950-2100 for six single model initial-condition large ensembles (SMILEs) in (a) September and (b) March. The bold line represents the ensemble-mean of each SMILE and the shading represents the range of each SMILE under historical and RCP8.5 forcing. The colored dotted lines represent the RCP scenarios from CMIP5 (shown only for the MPI-GE). The black vertical lines at 1950 and 2100 represent the spread from the 30 CMIP5 simulations. (c-d) Fractional contribution of model structure, emissions scenario, and internal variability to total uncertainty for the percent of remaining Arctic sea ice cover in (c) September and (d) March. The solid white lines denote the borders between each source of uncertainty, while the transparent white shading around those lines is the range of this estimate based on different estimates of internal variability in the MMLEA. Both fractional uncertainty panels are for five-year mean projections of percent of remaining Arctic sea-ice cover relative to 1995-2014.

189

190 These results suggest that uncertainty in short-term projections of Arctic sea ice,
 191 regardless of the season, is dominated by internal variability, while for long-term
 192 projections of Arctic sea ice, both scenario and model uncertainty become important. At
 193 long lead times, scenario uncertainty accounts for most of the uncertainty in projections
 194 of Arctic SIE in the summer months and model uncertainty accounts for most of the
 195 uncertainty in projections of Arctic SIE in the winter months. This likely reflects the
 196 fact that September Arctic SIE disappears in most GCMs by 2100 under RCP8.5.

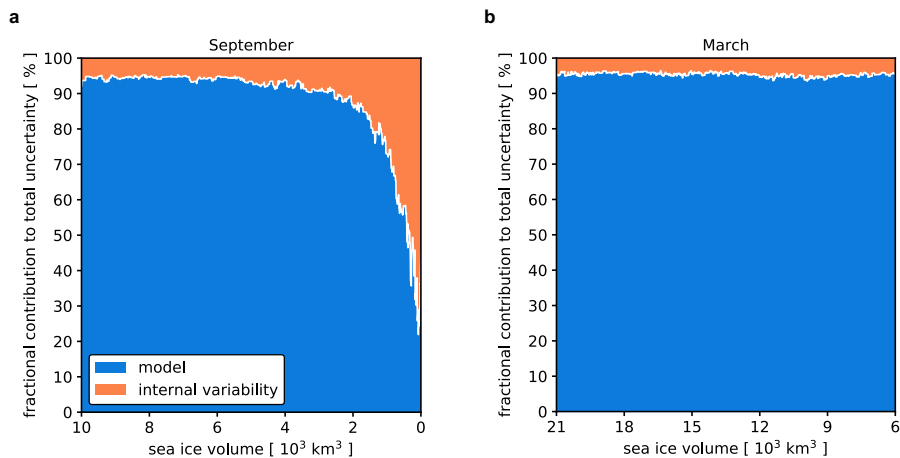


Figure 2. Fractional contribution of model structure and internal variability to total uncertainty for Arctic sea-ice extent (SIE) in (a) September and (b) March as a function of Arctic sea-ice volume (SIV). The solid white lines denotes the border between the two sources of uncertainty. Both fractional uncertainty panels are for projections of Arctic sea-ice extent with no temporal averaging or reference period. Note the x -axis is different for (a) and (b).

197 3.2. State dependence of internal variability

198 These results show a clear time-scale dependence for the relative importance of inter-
 199 nal variability in uncertainty of projections of Arctic SIE. However, recent studies have
 200 shown that the internal variability and the predictability of Arctic sea ice can change
 201 over time and under anthropogenic forcing (Goosse et al., 2009; Mioduszewski et al.,
 202 2019; Holland et al., 2019). September Arctic SIE variability is expected to increase
 203 under warming (Goosse et al., 2009; Mioduszewski et al., 2019), suggesting that the role
 204 of internal variability in sea ice projections is mean-state dependent. To investigate the
 205 role of internal variability in projections of Arctic sea ice as a function of the mean-state,
 206 we partition the relative sources of uncertainty with respect to SIV by binning a given
 207 SIE to its associated SIV for each month. We then perform the same variance analysis
 208 described above as a function of SIV instead of as a function of time. Doing this for
 209 each SMILE member and the ensemble-mean of each SMILE allows us to examine the

210 contributing sources of uncertainty as a function of SIV.

211

212 Figure 2 shows the fractional contribution of internal variability and model structure
 213 to total uncertainty for future Arctic SIE in September and March as a function of
 214 September and March Arctic SIV, respectively. Note, scenario uncertainty was excluded
 215 in these calculations (by using simulations from RCP 8.5 only) to isolate the effect of
 216 internal variability at different mean-states with respect to model uncertainty under
 217 the same mean-state. In September, as SIV declines — which is expected to occur
 218 throughout the 21st century — internal variability remains constant for most SIV
 219 values, accounting for approximately 10% of total uncertainty. However, at lower SIV
 220 regimes ($< 3,000 \text{ km}^3$), the contribution of internal variability increases and accounts
 221 for approximately 80% of the total uncertainty at low thickness sea ice regimes (i.e.,
 222 $\text{SIV} < 1,000 \text{ km}^3$). This is consistent with previous work that has shown increased
 223 variability of summer Arctic SIE as it approaches zero (e.g., Mioduszewski et al., 2019).
 224 In March, the contribution of internal variability to total uncertainty remains relatively
 225 constant at all SIV regimes, likely reflecting the fact that sea ice is present in most
 226 winter climates in future projections (e.g., Goosse et al., 2009). It is important to note
 227 that this increase in the contribution of internal variability to uncertainty at lower SIV
 228 regimes holds for summer (June, July, and August) months (not shown).

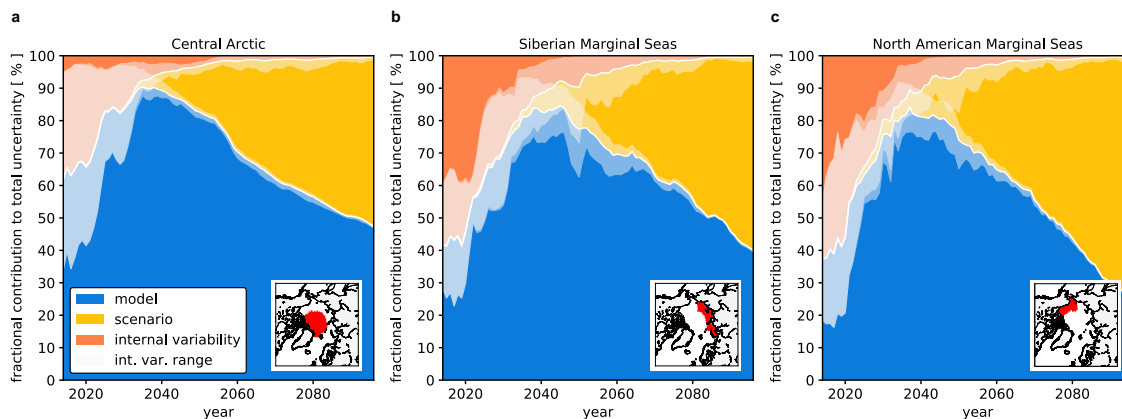


Figure 3. Fractional contribution of model structure, emissions scenario, and internal variability to total uncertainty for percent of remaining sea ice cover in July, August and September (JAS) for the Central Arctic, Siberian Marginal Seas (Kara Sea, Laptev Sea, East Siberian Sea), and North American Marginal Seas (Chukchi Sea, Beaufort Sea, Canadian Archipelago). The solid white lines indicate the borders between sources of uncertainty, while the transparent white shading around those lines is the range of this estimate based on different estimates of internal variability in the MMLEA. All panels are for five-year mean projections of percent of remaining Arctic sea-ice cover relative to 1995-2014.

229 3.3. Regional Arctic sea-ice extent

230 While the loss of total Arctic SIE is important for understanding the global climate re-
 231 sponse, climate change and sea ice loss are experienced predominately at regional scales
 232 (Barnhart et al., 2014; Lehner and Stocker, 2015). To investigate uncertainty in regional
 233 SIE projections, we compute SIE for 6 Arctic regions, which include the Central Arctic,
 234 Siberian Marginal Seas, North American Marginal Seas, Baffin/Hudson Bay and the
 235 Labrador Sea, the Bering Sea and Sea of Okhotsk, and Greenland-Iceland-Norwegian
 236 (GIN) and Bering Seas. These regions were chosen to represent geographically distinct
 237 parts of the Arctic ocean, where SIE retreat occurs with different velocities. As with
 238 total Arctic SIE, the SMILEs used in this study are found to be reasonably representa-
 239 tive of the CMIP5 inter-model spread for the percent of remaining Arctic sea ice cover
 240 in each region (see Figure S3).

241

242 Figure 3 shows the fractional contribution of each source of uncertainty to total uncer-
 243 tainty in projections of July, August, and September (JAS) SIE in the Central Arctic
 244 (Fig. 3a), Siberian Marginal Seas (Fig. 3b), and North American Marginal Seas (Fig.
 245 3c). We only show summertime SIE as these regions are fully ice covered in the winter-
 246 time and exhibit little wintertime variability throughout much of the 21st century. As
 247 with total September Arctic SIE, there is a large role for internal variability initially,
 248 accounting for as much as 80% of total uncertainty in the Siberian and North American
 249 Marginal Seas (Fig. 3b and 3b) and 60% in the Central Arctic (Fig. 3a). However, over
 250 time model uncertainty increases and eventually dominates for the first half of the 21st
 251 century in Central Arctic (Fig. 3a) and marginal seas (Fig. 3b and Fig. 3c), accounting
 252 for 40-50% of the total uncertainty. Note, the contribution of model structure to total
 253 uncertainty at the end of the century is lowest for the North American Marginal Seas.
 254 By the end of the 21st century scenario uncertainty dominates and accounts for over
 255 half of the uncertainty, meaning that whether or not an ice free Arctic occurs in the
 256 summertime is a direct consequence of climate change policy. Notably, the range of
 257 simulated internal variability contributions remain quite large through the 21st century
 258 in each region.

259

260 Figure 4 shows the fractional contribution of each source of uncertainty to total uncer-
 261 tainty in projections of January, February, and March (JFM) Arctic SIE in Baffin Bay,
 262 Hudson Bay and the Labrador Sea (Fig. 4a), Bering Sea and Sea of Okhotsk (Fig. 4b),
 263 and GIN and Barents Seas (Fig. 4c). These regions were selected to examine wintertime
 264 SIE as there is highly variable SIE in winter and little-to-no SIE in summer. As with
 265 regions of variable summer sea ice cover, these regions show a distinct pattern of un-
 266 certainty partitioning. For Baffin Bay, Hudson Bay, and Labrador Sea, approximately
 267 80% of total uncertainty in the next few decades is attributable to internal variability.
 268 Note that the contribution of uncertainty in the estimate of internal variability itself
 269 can cause this to change to only 20% (mainly driven by CSIRO-Mk3.6.0, which clearly

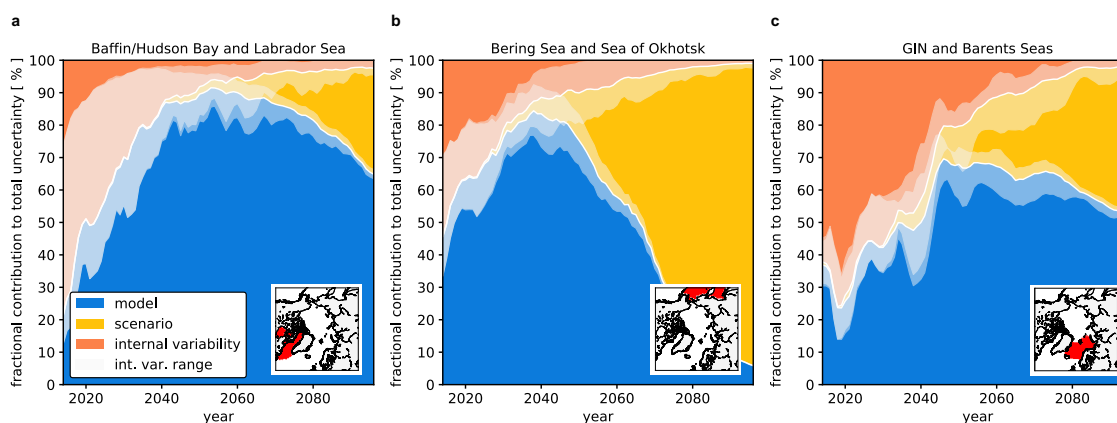


Figure 4. Fractional contribution of model structure, emissions scenario, and internal variability to total uncertainty for percent of remaining sea ice cover in January, February, and March (JFM) for (a) Baffin Bay, Hudson Bay, and the Labrador Sea, (b) Being Sea and Sea of Okhotsk, and the (c) GIN and Barents Seas. The solid white lines indicate the borders between sources of uncertainty, while the transparent white shading around those lines is the range of this estimate based on different estimates of internal variability in the MMLEA. All panels are for five-year mean projections of percent of remaining Arctic sea-ice cover relative to 1995-2014.

270 overestimates sea-ice extent in this region and Arctic-wide). The internal variability
 271 contribution diminishes to approximately 10% by the end of the century, and model
 272 structure dominates by 2030. A similar picture emerges for the Bering Sea and Sea
 273 of Okhotsk, but instead scenario uncertainty dominates in the latter half of the 21st
 274 century. Interestingly, the uncertainty partitioning for the GIN and Barents Seas has a
 275 distinct structure: internal variability dominates projection uncertainty for the next 30
 276 years and remains persistent throughout much of the 21st century. The contribution of
 277 internal variability is notably larger than in other regions and is most likely related to
 278 the influence of Atlantic heat transport on sea ice (Årthun et al., 2012).

279

280 A key result here — in contrast to total Arctic SIE for March and September — is
 281 the larger role of internal variability in contributing to total uncertainty, which persists
 282 throughout much of the 21st century. This suggests decadal predictions of regional
 283 Arctic SIE will be highly influenced by internal variability, especially for wintertime
 284 conditions in the GIN and Barents Seas. Moreover, the range of internal variability
 285 across models presents a unique challenge as internal variability could account for as
 286 much as 80% or as little as 20% of the total uncertainty in regions like the Labrador Sea
 287 in the coming decades. Understanding the cause of the range in this internal variability
 288 uncertainty is an important next step, whether it is related to model biases or dependent
 289 on the sea ice mean-state.

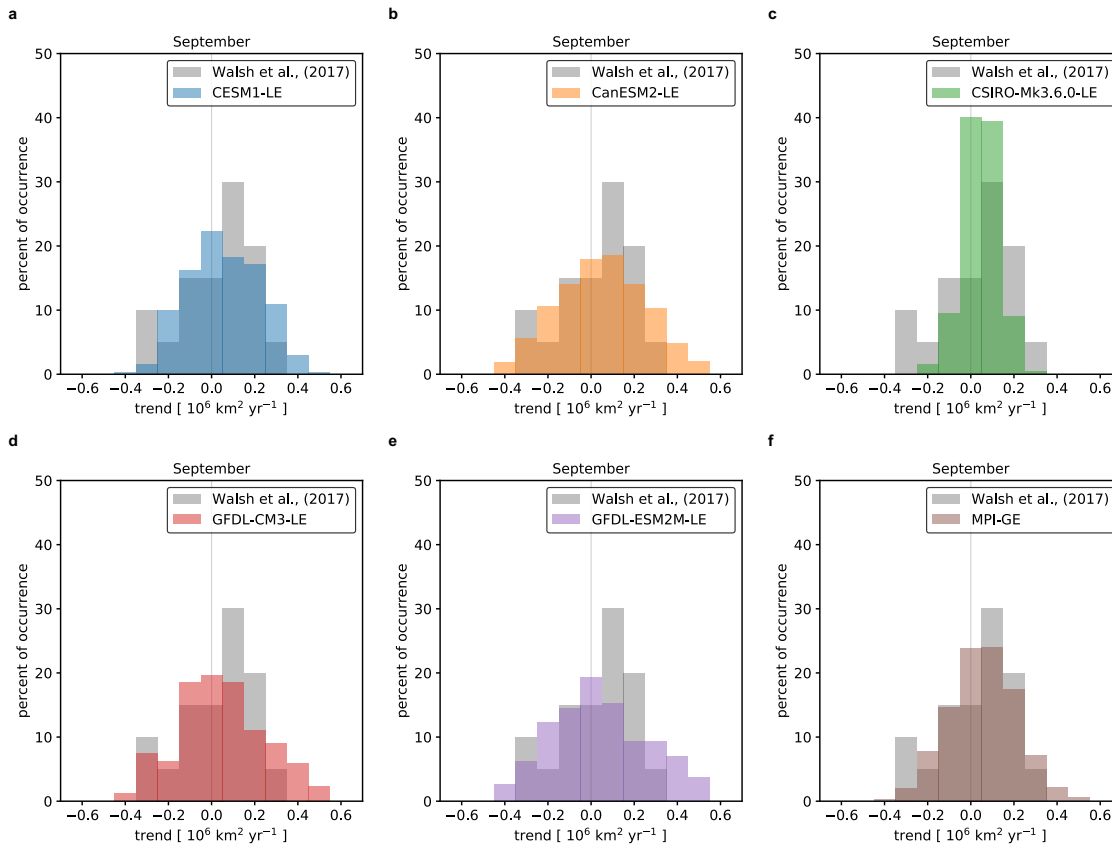


Figure 5. Percent of occurrence of separate 5-year trends in September Arctic sea-ice extent (SIE) from 1950-2019 for the (a) CESM1-LE, (b) CanESM2-LE, (c) CSIRO-Mk3.6.0-LE, (d) GFDL-CM3-LE, (e) GFDL-ESM2M-LE, and (f) MPI-GE. A 4th order polynomial was removed from each member of each SMILE prior to trend calculations to estimate the forced response. The bars show the distribution of trends for all members. The grey bars show percent of occurrence of separate 5-year trends in September Arctic SIE from 1930-2019 as estimated from Walsh et al. (2017). A 4th order polynomial was removed from the dataset prior to trend calculations to estimate the forced response.

290 4. Concluding remarks

291 The impacts of Arctic sea ice loss will be predominately felt by coastal communities,
 292 making it crucial to quantify and reduce projection uncertainty at regional scales. Here,
 293 we used a suite of SMILEs to investigate the sources of uncertainty in projections of
 294 Arctic SIE. For September SIE, model structure contributes between 40-80% of the total
 295 uncertainty over the next century, while for March SIE, model structure contributes ap-
 296 proximately 40-90% of the total uncertainty over the next century and accounts for more
 297 uncertainty at the end of the 21st century. We find a clear timescale dependence for
 298 internal variability. For September SIE, internal variability contributes approximately
 299 20-60% of total uncertainty in the next few decades, while for March SIE — and winter
 300 SIE more generally — internal variability contributes between 50-60% of total uncer-

301 tainty and influences projections at longer lead times. Scenario uncertainty contributes
302 mainly to uncertainty in summertime projections, accounting for approximately 70%
303 of total uncertainty by the end of the century. We also find that the role for internal
304 variability is mean-state dependent with thinner summer sea ice regimes more heavily
305 influenced by internal variability, accounting for approximately 80% of total uncertainty
306 for $SIV < 1,000 \text{ km}^3$. At regional scales, the contribution of internal variability to total
307 uncertainty increases, but has a large range and strongly depends on the month and
308 region. In the GIN and Barents Seas, for instance, internal variability contributes ap-
309 proximately 50-70% of the total uncertainty over the next 30 years, while for the Central
310 Arctic, internal variability accounts for approximately 20-30% of the total uncertainty.
311 This is likely related to the influence of Atlantic heat transport on sea ice in the North
312 Atlantic during the wintertime.

313

314 A unique result of our analysis is the partitioning of uncertainty due to different es-
315 timates of internal variability, which varies considerably across GCMs. This suggests
316 that at least some GCMs are biased in their magnitude of variability. Due to the short
317 observational record, it is difficult to precisely estimate the real-world magnitude of
318 SIE internal variability (e.g., Brennan et al., 2020). However, using a reconstruction
319 of September Arctic SIE to 1850 (Walsh et al., 2017) we try and estimate historical
320 Arctic SIE variability. We limit our analysis to 1930 due to sparse data coverage in
321 the Arctic prior to the 1930s. Figure 5 shows histograms of separate 5-year trends in
322 September Arctic SIE from 1950-2019 using all members of each SMILE. A 4th order
323 polynomial was used to approximate and remove the forced response to be consistent
324 with comparison to observations. The grey bars indicate the range from Walsh et al.
325 (2017) using separate 5-year trends from 1930 to 2019 after approximating the forced
326 response as a 4th order polynomial fit and removing it. While most models appear to
327 span the range of internal variability in the historical record, CSIRO-Mk3.6.0 does not
328 simulate a large enough range of 5-year trends, most likely reflecting the fact that sea ice
329 is biased high throughout the summer. This suggests the lowest contribution of internal
330 variability to total uncertainty in projections September Arctic SIE is likely not realis-
331 tic. Understanding and resolving these biases in internal variability across fully-coupled
332 GCMs should remain a focus of the sea ice community as it is important for attribution
333 of observed sea ice loss to anthropogenic climate change as well as for efforts of decadal
334 prediction.

335

336 Recent work has highlighted the role of remote internal processes in determining sea
337 ice trends across these same SMILEs (Topál et al., 2020), but a more process-oriented
338 analysis of the spatial and temporal timescales of this variability may better reveal the
339 sources of inter-model spread. For instance, it has been shown that these remote pro-
340 cesses are not stable on longer time scales (Bonan and Blanchard-Wrigglesworth, 2020),
341 suggesting that associated variability in September SIE during the satellite era does not
342 paint a complete picture of the future SIE variability. The outsized role for internal vari-

343 ability in projections of Arctic sea ice changes in the coming decades further motivates
344 the use of SMILEs to investigate a wide range of possible sequences of sea ice internal
345 variability and its drivers. However, such work is beyond the scope of this paper, whose
346 primary goal is to highlight the relative contribution of different sources of uncertainty
347 to Arctic sea ice projections at different spatial and temporal scales.

348

349 While internal variability poses a great challenge for predicting Arctic SIE in the
350 coming decades, the contribution of model structure to total uncertainty should not be
351 ignored. So-called “emergent constraints”, which link the inter-model spread in climate
352 projections to observable predictors, should be used when characterizing projection
353 uncertainty. Previous work has related the amount of future ice loss to the magnitude
354 of historical SIE trends (Boé et al., 2009; Hall et al., 2019) and to the initial state of the
355 sea ice (Bitz, 2008; Massonnet et al., 2012; Hall et al., 2019) and the Arctic climate
356 (Senftleben et al., 2020), but open questions remain as to why these relationships
357 exist and persist throughout the next century. Understanding biases in these trends
358 (e.g., Rosenblum and Eisenman, 2016, 2017) and the physical mechanisms behind these
359 constraints will improve the reliability of sea ice projections and increase confidence in
360 our understanding of what controls Arctic sea ice loss.

361 Acknowledgements

362 The authors thank the US CLIVAR Working Group on Large Ensembles for making
363 the large ensemble data publicly available, which can be found at the Multi-
364 Model Large Ensemble Archive (<http://www.cesm.ucar.edu/projects/community-projects/MMLEA/>). The authors also thank the climate modeling groups for producing
365 and making available their model output, which is accessible at the Earth System Grid
366 Federation (ESGF) Portal (<https://esgf-node.llnl.gov/search/cmip5/>). This work was
367 greatly improved through discussions with Mitch Bushuk and comments from Tapio
368 Schneider and Katie Brennan. D.B.B. was supported by an American Meteorological
369 Society (AMS) Graduate Fellowship.

371 References

- 372 1. Årthun, M., Eldevik, T., Smedsrud, L., Skagseth, Ø., and Ingvaldsen, R. (2012). Quantifying
373 the influence of Atlantic heat on Barents Sea ice variability and retreat. *Journal of Climate*,
374 25(13):4736–4743.
- 375 2. Barnhart, K. R., Miller, C. R., Overeem, I., and Kay, J. E. (2016). Mapping the future expansion
376 of Arctic open water. *Nature Climate Change*, 6(3):280–285.
- 377 3. Barnhart, K. R., Overeem, I., and Anderson, R. S. (2014). The effect of changing sea ice on the
378 physical vulnerability of Arctic coasts. *Cryosphere*, 8(5).
- 379 4. Bitz, C. M. (2008). Some aspects of uncertainty in predicting sea ice thinning. *Arctic Sea Ice*
380 *Decline: Observations, Projections, Mechanisms, and Implications*, *Geophys. Monogr.* 180:63–76.

- 381 5. Blanchard-Wrigglesworth, E., Armour, K. C., Bitz, C. M., and DeWeaver, E. (2011a). Persistence
382 and inherent predictability of Arctic sea ice in a GCM ensemble and observations. *Journal of*
383 *Climate*, 24(1):231–250.
- 384 6. Blanchard-Wrigglesworth, E., Bitz, C., and Holland, M. (2011b). Influence of initial conditions
385 and climate forcing on predicting Arctic sea ice. *Geophysical Research Letters*, 38(18).
- 386 7. Boé, J., Hall, A., and Qu, X. (2009). September sea-ice cover in the Arctic Ocean projected to
387 vanish by 2100. *Nature Geoscience*, 2(5):341–343.
- 388 8. Bonan, D. B. and Blanchard-Wrigglesworth, E. (2020). Nonstationary teleconnection between the
389 Pacific Ocean and Arctic sea ice. *Geophysical Research Letters*, 47(2):e2019GL085666.
- 390 9. Bonan, D. B., Christian, J. E., and Christianson, K. (2019). Influence of North Atlantic climate
391 variability on glacier mass balance in Norway, Sweden and Svalbard. *Journal of Glaciology*,
392 65(252):580–594.
- 393 10. Brennan, M. K., Hakim, G. J., and Blanchard-Wrigglesworth, E. (2020). Arctic Sea-Ice Variability
394 During the Instrumental Era. *Geophysical Research Letters*, 47(7):e2019GL086843.
- 395 11. Bushuk, M., Msadek, R., Winton, M., Vecchi, G., Yang, X., Rosati, A., and Gudgel, R. (2019).
396 Regional Arctic sea-ice prediction: potential versus operational seasonal forecast skill. *Climate*
397 *Dynamics*, 52(5-6):2721–2743.
- 398 12. Deser, C., Lehner, F., Rodgers, K., Ault, T., Delworth, T., DiNezio, P., Fiore, A., Frankignoul,
399 C., Fyfe, J., Horton, D., et al. (2020). Insights from Earth system model initial-condition large
400 ensembles and future prospects. *Nature Climate Change*, pages 1–10.
- 401 13. Deser, C., Phillips, A., Bourdette, V., and Teng, H. (2012). Uncertainty in climate change
402 projections: the role of internal variability. *Climate dynamics*, 38(3-4):527–546.
- 403 14. Deser, C., Terray, L., and Phillips, A. S. (2016). Forced and internal components of winter air
404 temperature trends over North America during the past 50 years: Mechanisms and implications.
405 *Journal of Climate*, 29(6):2237–2258.
- 406 15. Ding, Q., Schweiger, A., LHeureux, M., Battisti, D. S., Po-Chedley, S., Johnson, N. C., Blanchard-
407 Wrigglesworth, E., Harnos, K., Zhang, Q., Eastman, R., et al. (2017). Influence of high-latitude
408 atmospheric circulation changes on summertime Arctic sea ice. *Nature Climate Change*, 7(4):289–
409 295.
- 410 16. Ding, Q., Schweiger, A., LHeureux, M., Steig, E. J., Battisti, D. S., Johnson, N. C., Blanchard-
411 Wrigglesworth, E., Po-Chedley, S., Zhang, Q., Harnos, K., et al. (2019). Fingerprints of internal
412 drivers of Arctic sea ice loss in observations and model simulations. *Nature Geoscience*, 12(1):28–
413 33.
- 414 17. Eicken, H. (2013). Arctic sea ice needs better forecasts. *Nature*, 497(7450):431–433.
- 415 18. England, M., Jahn, A., and Polvani, L. (2019). Nonuniform contribution of internal variability to
416 recent Arctic sea ice loss. *Journal of Climate*, 32(13):4039–4053.
- 417 19. Goosse, H., Arzel, O., Bitz, C. M., de Montety, A., and Vancoppenolle, M. (2009). Increased
418 variability of the Arctic summer ice extent in a warmer climate. *Geophysical Research Letters*,
419 36(23).
- 420 20. Guemas, V., Blanchard-Wrigglesworth, E., Chevallier, M., Day, J. J., Déqué, M., Doblus-Reyes,
421 F. J., Fučkar, N. S., Germe, A., Hawkins, E., Keeley, S., et al. (2016). A review on Arctic sea-ice
422 predictability and prediction on seasonal to decadal time-scales. *Quarterly Journal of the Royal*
423 *Meteorological Society*, 142(695):546–561.
- 424 21. Hall, A., Cox, P., Huntingford, C., and Klein, S. (2019). Progressing emergent constraints on
425 future climate change. *Nature Climate Change*, 9(4):269–278.
- 426 22. Hawkins, E. and Sutton, R. (2009). The potential to narrow uncertainty in regional climate
427 predictions. *Bulletin of the American Meteorological Society*, 90(8):1095–1108.

- 428 23. Hawkins, E. and Sutton, R. (2011). The potential to narrow uncertainty in projections of regional
429 precipitation change. *Climate Dynamics*, 37(1-2):407–418.
- 430 24. Holland, M. M., Landrum, L., Bailey, D., and Vavrus, S. (2019). Changing Seasonal Predictability
431 of Arctic Summer Sea Ice Area in a Warming Climate. *Journal of Climate*, 32(16):4963–4979.
- 432 25. Jahn, A. (2018). Reduced probability of ice-free summers for 1.5 C compared to 2 C warming.
433 *Nature Climate Change*, 8(5):409–413.
- 434 26. Jahn, A., Kay, J. E., Holland, M. M., and Hall, D. M. (2016). How predictable is the timing of a
435 summer ice-free Arctic? *Geophysical Research Letters*, 43(17):9113–9120.
- 436 27. Jeffrey, S., Rotstayn, L., Collier, M., Dravitzki, S., Hamalainen, C., Moeseneder, C., Wong, K.,
437 and Syktus, J. (2013). Australias CMIP5 submission using the CSIRO-Mk3.6 model. *Aust.*
438 *Meteor. Oceanogr. J.*, 63:1–13.
- 439 28. Kay, J. E., Deser, C., Phillips, A., Mai, A., Hannay, C., Strand, G., Arblaster, J. M., Bates, S.,
440 Danabasoglu, G., Edwards, J., et al. (2015). The Community Earth System Model (CESM) large
441 ensemble project: A community resource for studying climate change in the presence of internal
442 climate variability. *Bulletin of the American Meteorological Society*, 96(8):1333–1349.
- 443 29. Kay, J. E., Holland, M. M., and Jahn, A. (2011). Inter-annual to multi-decadal Arctic sea ice
444 extent trends in a warming world. *Geophysical Research Letters*, 38(15).
- 445 30. Kirchmeier-Young, M. C., Zwiers, F. W., and Gillett, N. P. (2017). Attribution of extreme events
446 in Arctic sea ice extent. *Journal of Climate*, 30(2):553–571.
- 447 31. Koenigk, T., Beatty, C. K., Caian, M., Döscher, R., and Wyser, K. (2012). Potential decadal
448 predictability and its sensitivity to sea ice albedo parameterization in a global coupled model.
449 *Climate dynamics*, 38(11-12):2389–2408.
- 450 32. Landrum, L. and Holland, M. M. (2020). Extremes become routine in an emerging new Arctic.
451 *Nature Climate Change*, (<https://doi.org/10.1038/s41558-020-0892-z>).
- 452 33. Lehner, F., Deser, C., Maher, N., Marotzke, J., Fischer, E. M., Brunner, L., Knutti, R., and
453 Hawkins, E. (2020). Partitioning climate projection uncertainty with multiple large ensembles
454 and CMIP5/6. *Earth System Dynamics*, 11(2):491–508.
- 455 34. Lehner, F., Deser, C., and Terray, L. (2017). Toward a new estimate of time of emergence of
456 anthropogenic warming: Insights from dynamical adjustment and a large initial-condition model
457 ensemble. *Journal of Climate*, 30(19):7739–7756.
- 458 35. Lehner, F. and Stocker, T. F. (2015). From local perception to global perspective. *Nature Climate*
459 *Change*, 5(8):731–734.
- 460 36. Lique, C., Holland, M. M., Dibike, Y. B., Lawrence, D. M., and Screen, J. A. (2016). Modeling
461 the Arctic freshwater system and its integration in the global system: Lessons learned and future
462 challenges. *Journal of Geophysical Research: Biogeosciences*, 121(3):540–566.
- 463 37. Lovenduski, N. S., McKinley, G. A., Fay, A. R., Lindsay, K., and Long, M. C. (2016). Partitioning
464 uncertainty in ocean carbon uptake projections: Internal variability, emission scenario, and model
465 structure. *Global Biogeochemical Cycles*, 30(9):1276–1287.
- 466 38. Maher, N., Lehner, F., and Marotzke, J. (2020). Quantifying the role of internal variability in the
467 climate we will observe in the coming decades. *Environmental Research Letters*, 15.
- 468 39. Maher, N., Milinski, S., Suarez-Gutierrez, L., Botzet, M., Kornbluh, L., Takano, Y., Kröger,
469 J., Ghosh, R., Hedemann, C., Li, C., et al. (2019). The Max Planck Institute grand ensemble-
470 enabling the exploration of climate system variability. *Journal of Advances in Modeling Earth*
471 *Systems*, 11:2050–2069.
- 472 40. Marzeion, B., Cogley, J. G., Richter, K., and Parkes, D. (2014). Attribution of global glacier mass
473 loss to anthropogenic and natural causes. *Science*, 345(6199):919–921.

- 474 41. Massonnet, F., Fichefet, T., Goosse, H., Bitz, C. M., Philippon-Berthier, G., Holland, M. M.,
475 and Barriat, P.-Y. (2012). Constraining projections of summer Arctic sea ice. *The Cryosphere*,
476 6(6):1383–1394.
- 477 42. Meehl, G. A., Goddard, L., Boer, G., Burgman, R., Branstator, G., Cassou, C., Corti, S.,
478 Danabasoglu, G., Doblas-Reyes, F., Hawkins, E., et al. (2014). Decadal climate prediction: an
479 update from the trenches. *Bulletin of the American Meteorological Society*, 95(2):243–267.
- 480 43. Meehl, G. A., Goddard, L., Murphy, J., Stouffer, R. J., Boer, G., Danabasoglu, G., Dixon, K.,
481 Giorgetta, M. A., Greene, A. M., Hawkins, E., et al. (2009). Decadal prediction: Can it be skillful?
482 *Bulletin of the American Meteorological Society*, 90(10):1467–1486.
- 483 44. Mioduszewski, J. R., Vavrus, S., Wang, M., Holland, M., and Landrum, L. (2019). Past and
484 future interannual variability in Arctic sea ice in coupled climate models. *Cryosphere*, 13(1).
- 485 45. Niederdrenk, A. L. and Notz, D. (2018). Arctic sea ice in a 1.5 C warmer world. *Geophysical*
486 *Research Letters*, 45(4):1963–1971.
- 487 46. Perovich, D. K. and Polashenski, C. (2012). Albedo evolution of seasonal Arctic sea ice.
488 *Geophysical Research Letters*, 39(8).
- 489 47. Rodgers, K. B., Lin, J., and Frölicher, T. L. (2015). Emergence of multiple ocean ecosystem
490 drivers in a large ensemble suite with an Earth system model. *Biogeosciences*, 12(11):3301–3320.
- 491 48. Rosenblum, E. and Eisenman, I. (2016). Faster Arctic sea ice retreat in CMIP5 than in CMIP3
492 due to volcanoes. *Journal of Climate*, 29(24):9179–9188.
- 493 49. Rosenblum, E. and Eisenman, I. (2017). Sea ice trends in climate models only accurate in runs
494 with biased global warming. *Journal of Climate*, 30(16):6265–6278.
- 495 50. Schlunegger, S., Rodgers, K. B., Sarmiento, J. L., Ilyina, T., Dunne, J., Takano, Y., Christian,
496 J., Long, M. C., Frölicher, T. L., Slater, R., et al. (2020). Time of Emergence & Large
497 Ensemble intercomparison for ocean biogeochemical trends. *Global Biogeochemical Cycles*, page
498 e2019GB006453.
- 499 51. Screen, J. and Deser, C. (2019). Pacific Ocean variability influences the time of emergence of a
500 seasonally ice-free Arctic Ocean. *Geophysical Research Letters*, 46(4):2222–2231.
- 501 52. Senftleben, D., Lauer, A., and Karpechko, A. (2020). Constraining uncertainties in CMIP5
502 projections of September Arctic sea ice extent with observations. *Journal of Climate*, 33(4):1487–
503 1503.
- 504 53. Sigmond, M., Fyfe, J. C., and Swart, N. C. (2018). Ice-free Arctic projections under the Paris
505 Agreement. *Nature Climate Change*, 8(5):404–408.
- 506 54. Siler, N., Proistosescu, C., and Po-Chedley, S. (2019). Natural variability has slowed the decline
507 in western US snowpack since the 1980s. *Geophysical Research Letters*, 46(1):346–355.
- 508 55. SIMIP (2020). Arctic Sea Ice in CMIP6. *Geophysical Research Letters*, 47(10):e2019GL086749.
- 509 56. Smoliak, B. V., Wallace, J. M., Lin, P., and Fu, Q. (2015). Dynamical adjustment of the Northern
510 Hemisphere surface air temperature field: Methodology and application to observations. *Journal*
511 *of Climate*, 28(4):1613–1629.
- 512 57. Stroeve, J., Holland, M. M., Meier, W., Scambos, T., and Serreze, M. (2007). Arctic sea ice
513 decline: Faster than forecast. *Geophysical research letters*, 34(9).
- 514 58. Stroeve, J., Markus, T., Boisvert, L., Miller, J., and Barrett, A. (2014). Changes in Arctic melt
515 season and implications for sea ice loss. *Geophysical Research Letters*, 41(4):1216–1225.
- 516 59. Stroeve, J. and Notz, D. (2018). Changing state of Arctic sea ice across all seasons. *Environmental*
517 *Research Letters*, 13(10):103001.
- 518 60. Sun, L., Alexander, M., and Deser, C. (2018). Evolution of the global coupled climate response to
519 Arctic sea ice loss during 1990–2090 and its contribution to climate change. *Journal of Climate*,
520 31(19):7823–7843.

- 521 61. Swart, N. C., Fyfe, J. C., Hawkins, E., Kay, J. E., and Jahn, A. (2015). Influence of internal
522 variability on Arctic sea-ice trends. *Nature Climate Change*, 5(2):86–89.
- 523 62. Taylor, K. E., Stouffer, R. J., and Meehl, G. A. (2012). An overview of CMIP5 and the experiment
524 design. *Bulletin of the American Meteorological Society*, 93(4):485–498.
- 525 63. Topál, D., Ding, Q., Mitchell, J., Baxter, I., Herein, M., Haszpra, T., Luo, R., and Li, Q.
526 (2020). An Internal Atmospheric Process Determining Summertime Arctic Sea Ice Melting in
527 the Next Three Decades: Lessons Learned from Five Large Ensembles and Multiple CMIP5
528 Climate Simulations. *Journal of Climate*, 33(17):7431–7454.
- 529 64. Wallace, J. M., Fu, Q., Smoliak, B. V., Lin, P., and Johanson, C. M. (2012). Simulated versus
530 observed patterns of warming over the extratropical Northern Hemisphere continents during the
531 cold season. *Proceedings of the National Academy of Sciences*, 109(36):14337–14342.
- 532 65. Walsh, J. E., Fetterer, F., Scott Stewart, J., and Chapman, W. L. (2017). A database for depicting
533 Arctic sea ice variations back to 1850. *Geographical Review*, 107(1):89–107.
- 534 66. Wang, M. and Overland, J. E. (2009). A sea ice free summer Arctic within 30 years? *Geophysical*
535 *research letters*, 36(7).
- 536 67. Yang, C.-Y., Liu, J., Hu, Y., Horton, R. M., Chen, L., and Cheng, X. (2016). Assessment of Arctic
537 and Antarctic sea ice predictability in CMIP5 decadal hindcasts. *Cryosphere*, 10(5):2429–2452.
- 538 68. Yeager, S. G., Karspeck, A. R., and Danabasoglu, G. (2015). Predicted slowdown in the rate of
539 Atlantic sea ice loss. *Geophysical Research Letters*, 42(24):10–704.
- 540 69. Zhang, R. (2015). Mechanisms for low-frequency variability of summer Arctic sea ice extent.
541 *Proceedings of the National Academy of Sciences*, 112(15):4570–4575.